JOURNAL OF GEOPHYSICAL RESEARCH, VOL. 108, NO. D6, 4192, doi:10.1029/2002JD002698, 2003

Statistical characteristics of the electric and magnetic fields and their time derivatives 15 m and 30 m from triggered lightning

J. Schoene, M. A. Uman, V. A. Rakov, V. Kodali, K. J. Rambo, and G. H. Schnetzer
Department of Electrical and Computer Engineering, University of Florida, Gainesville, Florida, USA

Received 25 June 2002; revised 1 November 2002; accepted 2 January 2003; published 28 March 2003.

[1] We present a statistical analysis of the salient characteristics of the electric and magnetic fields and their derivatives at distances of 15 m and 30 m from triggered lightning strokes that lowered negative charge to ground. Return stroke current and current derivative characteristics are also presented. The measurements were made during the summers of 1999 and 2000 at Camp Blanding, Florida. Lightning was triggered to a 1 to 2 m strike object at the center of a 70 m $\times$ 70 m metal-grid ground plane that was buried beneath a few centimeters of soil. The strike object was mounted on the rocket launching system that was located below ground level in a pit. The experiment was designed (1) to minimize the influence of the strike object on the field and field derivative waveforms an (2) to eliminate potential distortions of the field and field derivative waveforms both due to ground surface arcing and due to the propagation of the field being over imperfectly conducting ground. Measurements were made on about 100 return strokes, although not all field quantities were successfully recorded for each stroke. We present histograms and parameters of statistical distributions for the following 28 waveform characteristics: current peak, risetime, and width; current derivative peak, risetime, and width; return-stroke electric field change and field pulse width at 15 m and at 30 m; electric field derivative peak, risetime, and width at 15 m and at 30 m; magnetic field peak, risetime, and width at 15 m and at 30 m; and magnetic field derivative peak, risetime, and width at 15 m and at 30 m. We compare our results with those from previous studies. From this comparison we infer, among other results, that for strikes to our buried metal-grid ground plane the current risetime and width are, on average, smaller than for strikes to concentrated grounding electrodes (vertical ground rods). *INDEX TERMS:* 0619 Electromagnetics: Electromagnetic theory; 0634 Electromagnetics: Measurement and standards; 3304 Meteorology and Atmospheric Dynamics: Atmospheric electricity; 3324 Meteorology and Atmospheric Dynamics: Lightning; *KEYWORDS:* rocket-triggered lightning, electromagnetic environment, return stroke, statistical characteristics of lightning, electromagnetic fields, ICLRT

Citation: Schoene, J., M. A. Uman, V. A. Rakov, V. Kodali, K. J. Rambo, and G. H. Schnetzer, Statistical characteristics of the electric and magnetic fields and their time derivatives 15 m and 30 m from triggered lightning, *J. Geophys. Res.*, *108*(D6), 4192, doi:10.1029/2002JD002698, 2003.

1. Introduction

[2] Statistical characteristics of the electric and magnetic fields from very close lightning are needed for proper assessment of the hazard to objects and systems from these fields. Further, knowledge of the electric and magnetic fields very close to lightning is of interest for two reasons other than the hazard assessment: (1) the fields contain information on the physics of the processes by which lightning attaches to the ground, and (2) the fields can be used to evaluate existing return stroke models and to develop new ones. We present here the first phase of the statistical characterization of this very close lightning electromagnetic environment: the salient characteristics of the electric and magnetic field waveforms and the associated time derivative waveforms observed 15 m and 30 m from triggered lightning strokes. These strokes are thought to be similar to subsequent strokes (those after the first stroke) in natural cloud-to-ground flashes. The second phase of the statistical characterization of the close lightning electromagnetic environment, now underway, will involve the electric and magnetic fields of natural first strokes. Results of earlier studies of the close lightning electromagnetic environment are given by *Leteinturier et al.* [1990], *Depasse* [1994], *Rubinstein et al.* [1995], *Rakov et al.* [1998], *Uman et al.* [2000], *Crawford et al.* [2001], *Miki et al.* [2002], and *Uman et al.* [2002].

[3] The field waveforms from triggered lightning strokes analyzed here were recorded in the summers of 1999 and

0148-0227/03/2002JD002698$09.00

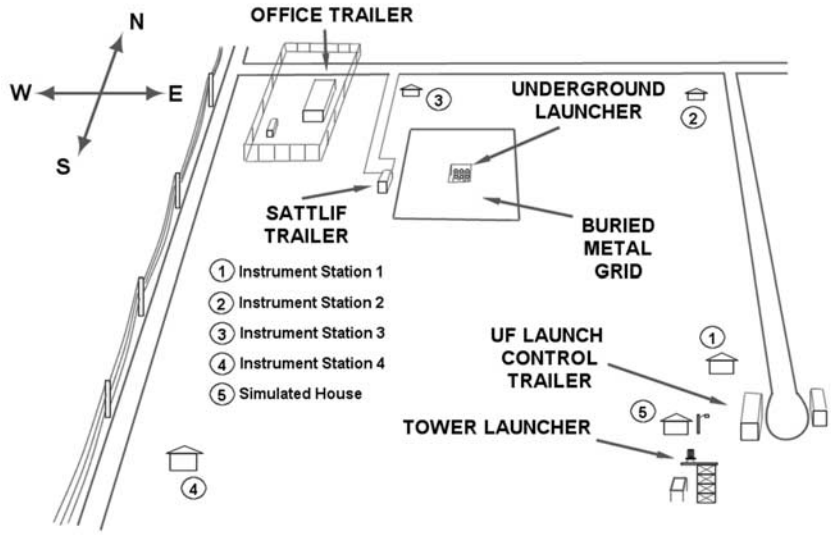

Figure 1. Sketch of the experimental site at Camp Blanding, 1999–2000. Not all test objects are shown.

2000 at the International Center for Lightning Research and Testing (ICLRT) at Camp Blanding in north central Florida, near Starke. In our experiments, the height of the strike object above ground was relatively small, 1 to 2 m, so as to minimize any effects of the strike object [*Uman et al.*, 2000], and all fields propagated from the strike point to the antenna over a buried metal grid intended to simulate a perfectly conducting ground plane so as to eliminate potential waveform distortion associated with field propagation over an imperfectly conducting earth [e.g., *Cooray and Lundquist*, 1983; *Cooray*, 1987]. Additionally, the metal grid was intended to suppress the electric arcs that often develop radially outward along the ground surface from the lightning strike point [*Rakov et al.*, 1998], and the grid apparently fulfilled this function.

[4] Electric field derivatives from triggered lightning were previously measured at Camp Blanding in 1998 at distances of 10, 14, and 30 m by *Uman et al.* [2000]. In these studies, the fields propagated over poorly conducting sandy soil, and a relatively high (compared to the present study) strike object of either 6 m or 10 m was used. Electric field derivative data at 50 m have been reported by *Leteinturier et al.* [1990] and *Weidman et al.* [1986] from a 1985 study at the Kennedy Space Center, Florida and a 1986 study at St. Privat d'Allier, France. These results and others have been summarized by *Uman et al.* [2000]. *Uman et al.* [2000] have inferred that the differences between the Kennedy Space Center electric field derivative waveforms reported by *Leteinturier et al.* [1990] and those observed at Camp Blanding during 1998 are associated with the tall, 20 m, rocket launching structure used at the Kennedy Space Center (a factor of two to three taller than at Camp Blanding), motivating, in part, our effort to employ the smallest possible strike object in the present study.

[5] *Uman et al.* [2002] have analyzed in detail the current and electric and magnetic field derivative waveforms of two triggered strokes from the 1999 campaign at Camp Blanding to address some aspects of the relation between the currents and fields when there is a small strike object and when field propagation is over a well-conducting ground plane. Those two strokes, labeled S9934-6 and S9934-7, are included in the present data set. *Uman et al.* [2002] describe the experimental setup for 1999 [see also *Crawford et al.*, 2001, section 2.4; *Rakov et al.*, 2001, section 2.2] and show that, for these two strokes, the transmission-line model [*Uman and McLain*, 1969] of the return stroke provides a fairly good representation of the relation between the waveforms and peak values of the measured current derivative and the measured electric and magnetic field derivatives at 15 m for assumed return stroke speeds between 2 and 3 $\times$ 10^8 m/s. They also show, using the transmission line model, that the similarity in the wave shape of these three derivatives for the first 150 ns or so does not require or imply a dominant radiation field, as had been previously suggested as a possible explanation [*Uman et al.*, 2000], but only a relatively high return stroke speed for the first 150 ns.

[6] In this paper, we show histograms, along with statistical summaries, for the following 28 salient parameters of the current and electric and magnetic field waveforms: current peak, risetime, and width; current derivative peak, risetime, and width; return stroke electric field change and field pulse width at 15 m and at 30 m; electric field derivative peak, risetime, and width at 15 m and at 30 m; magnetic field peak, risetime, and width at 15 m and at 30 m; and magnetic field derivative peak, risetime, and width at 15 m and at 30 m. The risetimes were measured between the 30% and 90% values of the peak on the initial rising portion of the return-stroke waveform, and the widths were measured at the half-peak level. We also compare our results with those obtained from other triggered-lightning experiments. All strokes analyzed here lowered negative charge to ground.

2. Experiment

[7] A sketch of the ICLRT during the 1999 and 2000 experiments is found in Figure 1. The rocket-and-wire technique was used to artificially initiate lightning from natural thunderclouds [e.g., *Rakov et al.*, 1998]. The rocket launcher consisted of six vertical metallic tubes mounted on

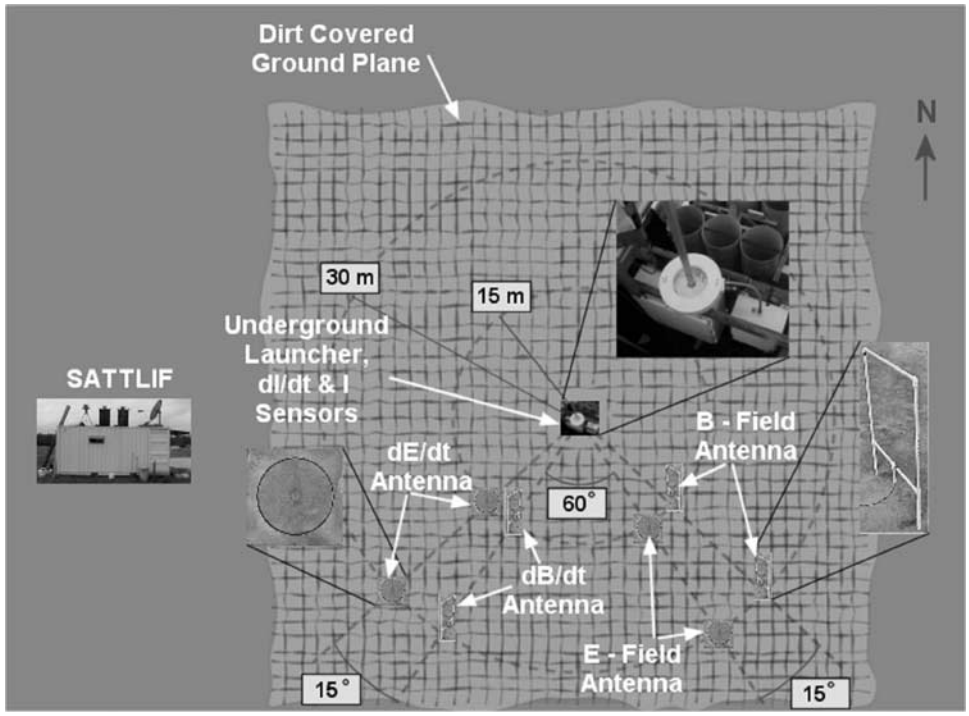

Figure 2. Underground launcher with the strike rod and current and current derivative measuring devices in the center of the buried metal grid with electric (E) and magnetic (B) field and field derivative (dE/dt and dB/dt) antennas at 15 and 30 m.

insulating fiberglass legs. The launcher was placed underground in the center of a 4 m × 4 m pit with the top of the launcher flush with the ground surface. The triggering rockets were launched at a small angle from the vertical, towards the east, to minimize the possibility that, in the case of an unsuccessful triggering attempt, a triggering wire would cross the power distribution line feeding the ICLRT, located to the west of the launcher. A hollow metal rod with an outside diameter of 3.8 cm and a wall thickness of 0.6 cm protruding one meter above the ground surface was used as the strike object in 1999 for flashes S9901–S9918. For the remainder of 1999 the rod length was changed to two meters in order to increase the probability of lightning attachment to the rod. In 2000, the strike object was a 2 m vertical rod surrounded by a 3 m diameter horizontal ring elevated to 1.5 m height and electrically connected to the base of the rod [*Miki et al.*, 2002, Figure 3]. The underground launcher was located at the center of a 70 m × 70 m metal grid that was covered by soil (sand). The mesh size of the grid was 5 cm × 10 cm. The low frequency, low current grounding resistance of the grid was measured to be 6 Ω. During 1999 the underground launcher was connected via four metal straps to the grid and the base of the launcher was connected via two metal straps to a 16.5 m long ground rod whose low frequency, low current grounding resistance was measured to be 40 Ω. For the 2000 studies, the launcher was connected by only two metal straps to the grid. A pneumatic control system operated from the Sandia Transportable Triggered Lightning Instrumentation Facility (SATTLIF) trailer was used to fire the rockets. Electric and magnetic fields and their time derivatives were measured with antennas located 15 m and 30 m from the strike rod. The locations of the antennas are shown in Figure 2. Figure 3 shows a photograph of the experimental site and of triggered lightning S0013.

[8] The SATTLIF digitizing system in 1999 and 2000 consisted of LeCroy models RM9400 and RM9400A digital storage oscilloscopes. Each of these oscilloscopes has two channels that can store 25 kilosamples with a sampling rate of up to 125 MHz (RM9400) or 175 MHz (RM9400A), with 8-bit amplitude resolution. The memory in the LeCroy oscilloscopes was segmented to allow eight triggers during a single lightning strike, each with 2501 sample points, and therefore signals from up to 8 events per flash could be recorded. Most of the events recorded in 1999 and 2000 were leader/return stroke sequences, but about 9 events were M component type

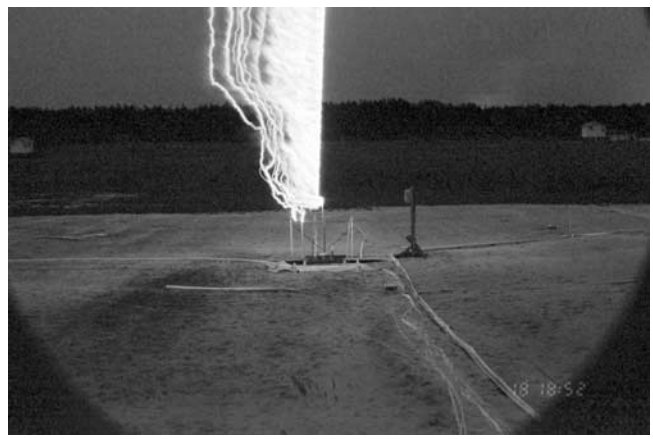

Figure 3. A photograph of the experimental site and triggered lightning S0013. The photograph was taken from the SATTLIF trailer.

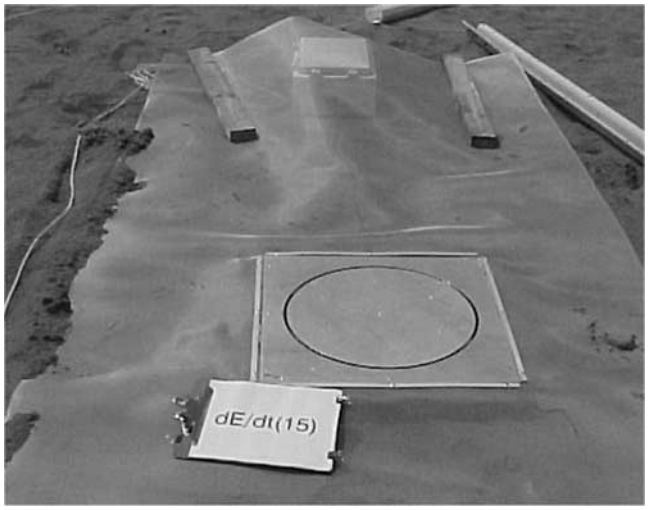

Figure 4. Flat-plate antenna for dE/dt measurement with Hoffmann box covered by metallic screen.

pulses [e.g., *Rakov et al.*, 2001]. The M component type pulses are not included in the statistics presented here.

[9] In 1999, a TTL-level digital pulse trigger signal was generated when the magnetic field sensor located 15 m from the rocket launcher detected a magnetic field that corresponded to a current of at least 5 kA (using Ampere's law of magnetostatics, $B = \mu_0 I/2\pi r$). In 2000, the TTL-level digital pulse trigger signal was generated when the current viewing resistor (CVR) installed at the strike rod base sensed a current that exceeded ±3.2 kA. The TTL signal was transmitted to the external trigger input of the SATTLIF oscilloscopes to trigger the digitizing system. The oscilloscopes for the field and current measurement had a pre-trigger (stored data recorded prior to the trigger pulse) that ranged from 10% to 50% of the total record length.

[10] Fiber optic transmitters (FOT) converted the analog output signals from the antennas to optical signals and transmitted those signals via fiber optic cables to fiber optic receivers (FOR). Meret and Nanofast fiber optic links (FOL) were used in the experiment. The bandwidth of the Meret and Nanofast FOL was dc to 35 MHz and 5 Hz to 175 MHz, respectively. The FOT were powered with 12 V dc lead-acid batteries. RG-58 or RG-223 coaxial cables (both 50 Ω) connected the FOT to the antennas, which were located in metal boxes near the antennas. The FORs in the SATTLIF trailer were powered with 120 V ac uninterruptible power supplies (UPS). RG-58 or RG-223 coaxial cables connected the FOR to the digitizing system. The optical fibers transmitting the signal from the FOT to the FOR were 200 μm glass, Kevlar-reinforced, duplex cables.

[11] A Pentax SG-10 automatic 35-mm camera with a 19 mm wide-angle lens was located inside the SATTLIF trailer in order to photograph the triggered flashes. A framing camera inside SATTLIF was employed for relatively high-speed recording of the triggered-lightning events. That camera was operated with a 1 ms exposure time at a framing rate of 200 frames/second, or a time resolution of 5 ms. An LED timing index flashing at a 100 Hz rate provided 10 ms timing marks for accurate timing. Three video cameras located so as to allow a three-dimensional reconstruction of the lightning channel were also used for recording triggered lightning events.

[12] In 1999, six P110A current transformers (CT) with a lower frequency response of 1 Hz and an upper frequency response of 20 MHz were used to measure the current at the channel base, two measured the current flow to the ground rod, and four measured the current flow to the grounding grid. The current amplitude range of each sensor is from a few amperes to approximately 20 kA. In 1999 a passive combiner summed the two signals from the ground rod CTs to obtain a total ground rod current and another one summed the four signals from the grounding grid CTs to obtain a total grid current. The total ground rod current signal and the total grid current signal were then each transmitted via separate Meret FOL (35 MHz bandwidth) to the SATTLIF facility. Both signals were filtered with a 20 MHz, 3 dB anti-aliasing filter and then digitized at 50 MHz. The total current at the channel base was obtained by numerically summing the ground rod current and the grounding grid current.

[13] The 2000 instrumentation for measuring current differed from that in 1999. The primary differences between the 1999 and the 2000 instrumentation were: (1) The 2000 current at the channel base was measured simultaneously by two different methods rather than by one as in 1999: (a) the total lightning current was measured using a single current viewing resistor installed just below the strike object, and (b) the strike object had two connections to the ground rod and two connections to the grounding grid at which currents were measured. The current to the ground rod was measured as in 1999, while the currents to the grounding grid were measured with two current viewing resistors in the two connections rather than with the four current transformers and four connections used in 1999.

[14] The current derivative, dI/dt, was measured with an EG&G IMM-5 I-Dot sensor with an upper frequency response of 300 MHz [*Baum*, 1986]. That sensor was located at the base of the strike rod. The dI/dt signal was transmitted via a Nanofast FOL (175 MHz bandwidth) to

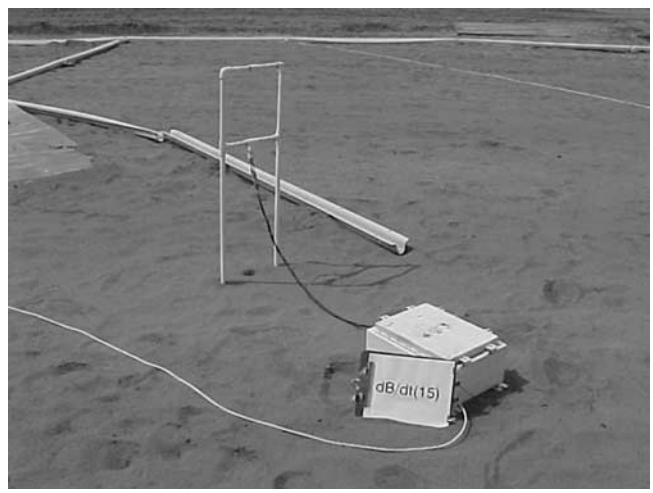

Figure 5. Rectangular loop antenna for dB/dt measurement with Hoffmann box containing fiber optic transmitter and battery. In the background are the PVC channels for the fiber optic cables.

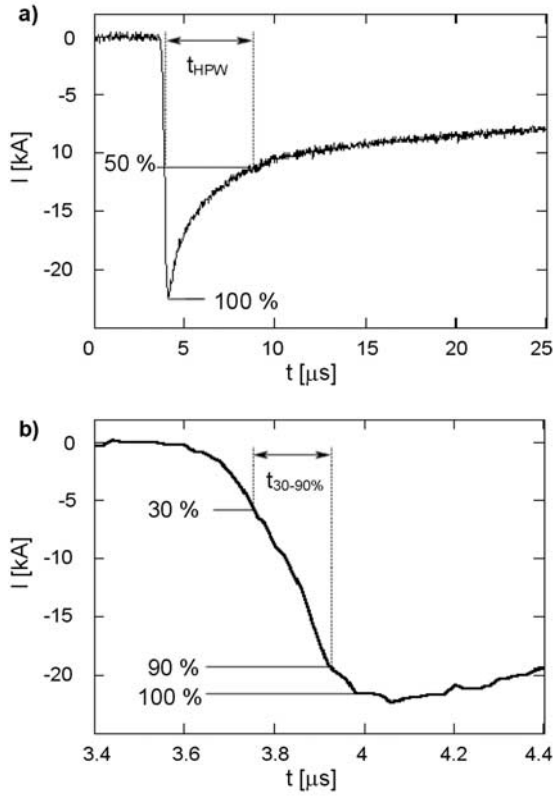

Figure 6. Current record of return stroke 2 of flash S9930 on a) 25 μs and b) 1 μs timescales. Half-peak width and 30–90% risetime measurements are illustrated in a) and b), respectively.

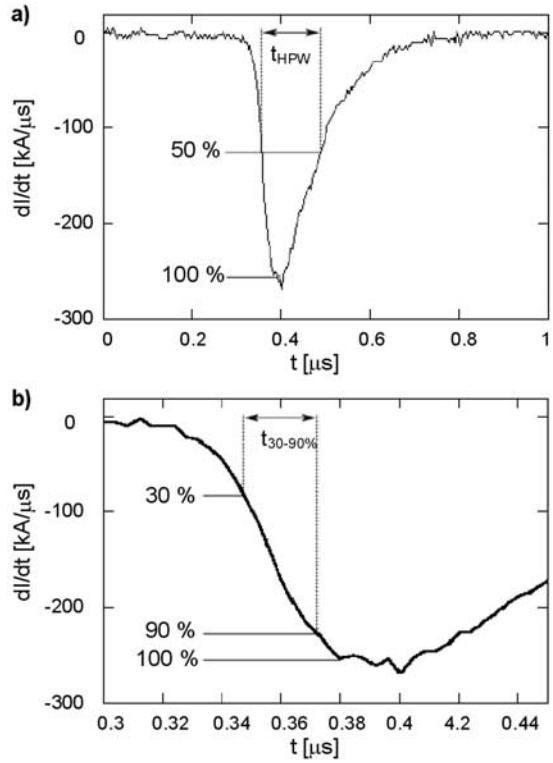

Figure 7. Current derivative record of return stroke 1 of flash S9934 on a) 1 μs and b) 0.15 μs timescales. Half-peak width and 30–90% risetime measurements are illustrated in a) and b), respectively.

the SATTLIF trailer where it was filtered with a 20 MHz, 3 dB anti-aliasing filter and then digitized at 250 MHz.

[15] Flat-plate antennas (0.16 m^2) were used for the electric field and electric field derivative measurements. The E-field antennas were connected to Meret fiber optic transmitters having an input impedance of about R_{in} = 1 MΩ. For the dE/dt measurement, a 50-Ω resistor was connected across the antenna terminals. For the E-field measurements at 15 m/30 m, integrating capacitors of C_{int} = 105 nF/C_{int} = 55 nF were used, resulting in decay time constants of 100 ms/50 ms. The rise time constant for the dE/dt antennas are determined by the antenna and system cabling capacitances, which are in the order of 100s of pF, resulting in a rise time constant of several ns. The housings of the flat plate antennas were electrically connected to the grounding grid. The electromagnetically shielded metal ''Hoffman'' enclosures (boxes) containing a fiber optic transmitter, a 12 V battery, and an integrating capacitor (E-field measurement)/terminating resistor (dE/dt measurement) were covered with metallic screens. The screens were fastened to the antenna housings. The function of the screen was to minimize electric field distortion by the antenna. Figure 4 shows the flat-plate antenna used to measure dE/dt at 15 m, as well as the Hoffman box covered with metallic screen.

[16] Meret fiber optic links with a 35 MHz bandwidth transmitted the signal to the digitizer from the E-field antenna at 15 m, the E-field antenna at 30 m, and the dE/dt antenna at 15 m. A Nanofast FOL was used for the dE/dt antenna at 30 m. The E-field signal recorded at 15 m was filtered with a 10 MHz, 3 dB low pass filter and then digitized at 25 MHz; the E-field signal recorded at 30 m was filtered with a 20 MHz, 3 dB low pass filter and then digitized at 25 MHz; and dE/dt signals recorded at both 15 and 30 m were

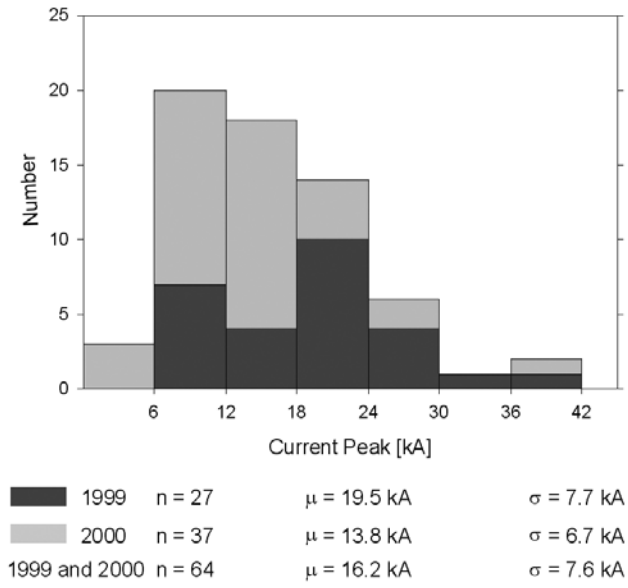

Figure 8. Histograms of current peaks. Data for 1999 and 2000 are shown stacked.

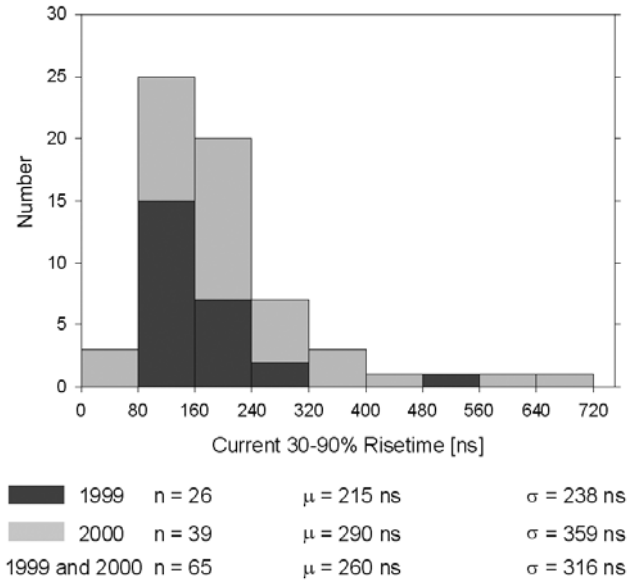

Figure 9. Histograms of current risetimes. Three values, 1300 ns (1999), and 1680 ns and 1750 ns (2000), are not shown in the histograms but are included in the statistics.

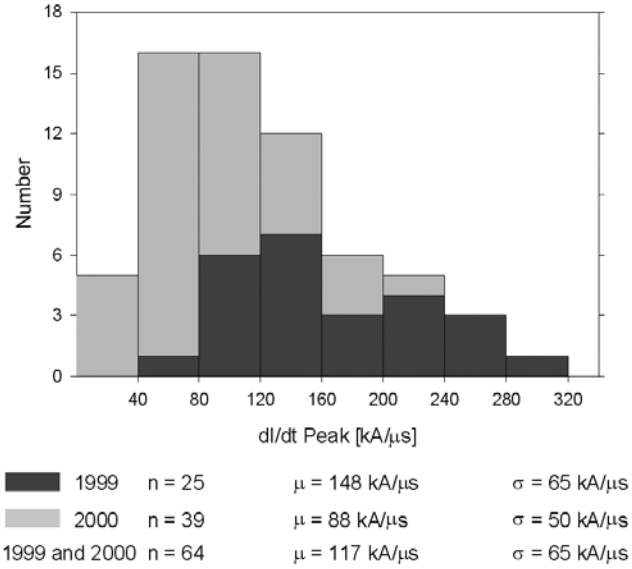

Figure 11. Histograms of dI/dt peaks. The dI/dt peaks from the 1999 experiment were obtained both from directly measured current derivative waveforms and differentiated current waveforms. The dI/dt peaks from the 2000 experiment were obtained from directly measured current derivative waveforms only.

filtered with 20 MHz, 3 dB low pass filters and then digitized at 250 MHz. The electric field and field derivative antennas were experimentally calibrated as described by *Uman et al.* [2000].

[17] Rectangular loop antennas with areas of 0.56 m^2 and 0.09 m^2 were used for the magnetic field and magnetic field derivative measurements, respectively. The measured loop inductance was about 4 μH for the magnetic field antenna and about 1.2 μH for the magnetic field derivative antenna. The magnetic field and magnetic field derivative loops (see Figure 5) had inserted series resistors of 50 Ω and 470 Ω, respectively, and both loop systems were terminated in 50 Ω.

An active integrator with a decay time constant of 1.5 ms and an effective bandwidth near 10 MHz was used for obtaining the B-field from the magnetic field derivative signal across the 50 Ω resistor of the magnetic field system. Meret fiber optic links with a 35 MHz bandwidth were used to transmit the signals from all four loop antennas to the digitizers. The magnetic field signals were filtered with 10 MHz, 3 dB anti-aliasing filters and then digitized at 25 MHz, and dB/dt signals at 15 and 30 m were filtered with 20 MHz, 3 dB anti-aliasing filters and then digitized at 250 MHz and 50 MHz, respectively. To test the high frequency response of the

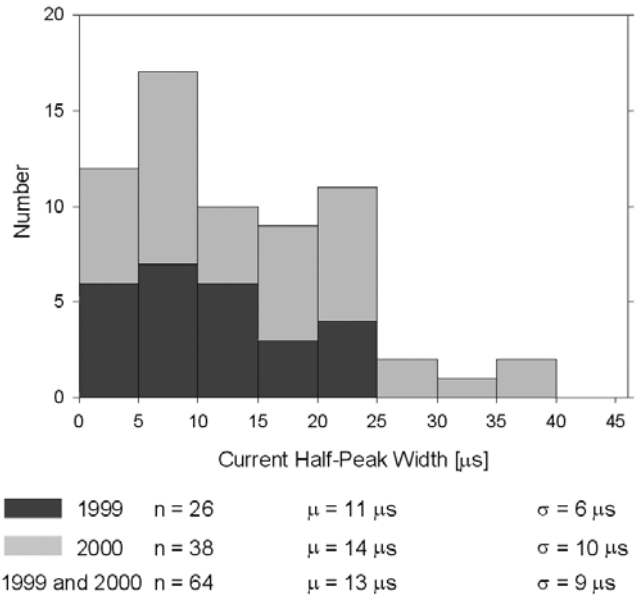

Figure 10. Histograms of current half-peak widths.

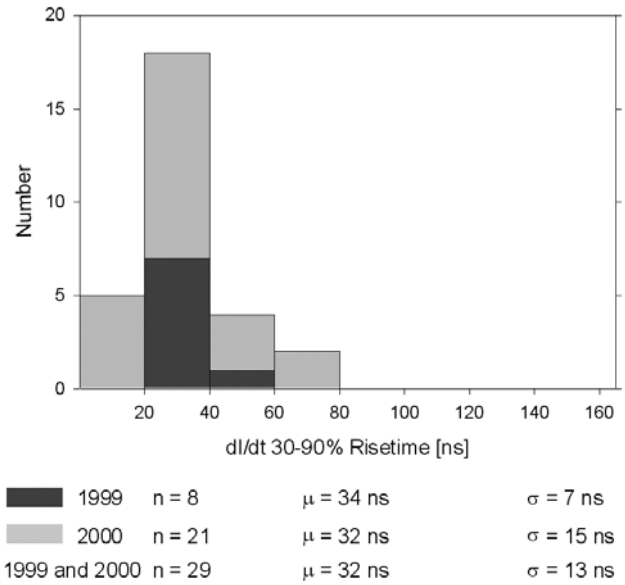

Figure 12. Histograms of current derivative risetimes.

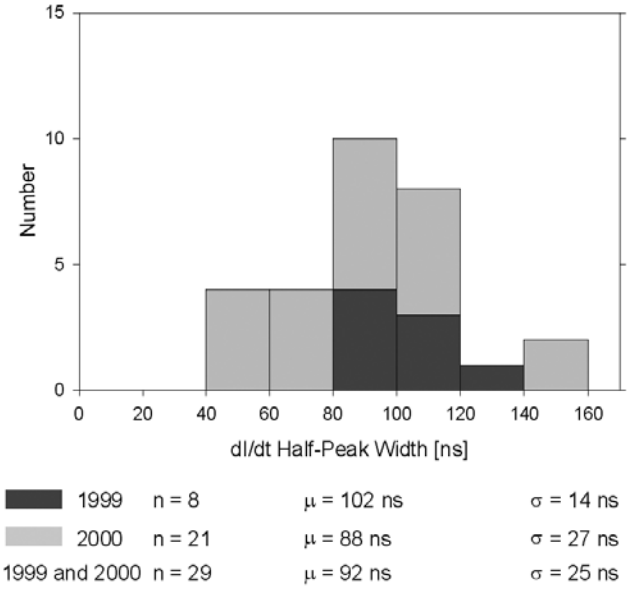

Figure 13. Histograms of current derivative half-peak widths.

magnetic field and magnetic field derivative antenna systems, we injected a fast rising current pulse into a Helmoltz Coil surrounding the antenna and measured the system output with and without the anti-aliasing filters attached. For the magnetic field derivative antenna the 10–90% risetime was 3 ns, and the risetime at the filter output was 13 ns. For the magnetic field antenna the 10–90% risetime before the integrator was 10 ns. For the Helmoltz Coil system used, the output of the integrator was too small to determine an accurate risetime, but separate measurements on the integrator and anti-aliasing filter indicate a total system risetime of less than 100 ns.

[18] In the data presentation to follow we indicate a horizontal distance of either 15 or 30 m from the antennas to the lightning. The optical data obtained with the instrumentation described above show that, for the 1999 experiment, the lightning attachment point was either at the top of the 1 m or 2 m high strike rod (36 of 53 strokes), on the rocket launcher, or on the edge of the 4 m × 4 m pit housing the rocket launcher. For the 2000 experiment, the lightning attachment point was always either at the top of the 2 m high strike rod or on the 1.5 m radius ring elevated 1.5 m above ground and centered on the 2 m rod. The channel above the attachment point is rarely straight or vertical (as noted earlier, the rocket is launched at a slight easterly angle from the vertical) and can be moved horizontally by the prevailing wind a distance of 1 m or more during the course of a flash. An example is shown in Figure 3. In this example, while the channel attachment point is always within 1.5 m of the "nominal" distances of 15 m or 30 m, depending on whether it is on the rod or on the surrounding ring, the channel above the attachment point is displaced up to several meters.

3. Data and Analysis

[19] The following analysis is based on data for about 100 strokes recorded in 1999 and 2000. Some parts of this data set were also used in studies published by *Crawford et al.* [2001], *Rakov et al.* [2001], *Uman et al.* [2002], and *Miki et al.* [2002]. Since the rockets were launched at a small angle from the vertical, toward the east (away from SATTLIF and away from the power line to the west of SATTLIF), most lightning channels were inclined to the east, and most were additionally affected by the prevailing winds. Since the electric and magnetic field antennas are located southeast of the strike point and the electric and magnetic field derivative antennas are located southwest of the strike object (Figure 2) our statistics are possibly biased towards slightly larger values for electric and magnetic field amplitudes and towards slightly smaller values for electric and magnetic field derivative peaks due to the average channel inclination to the east. Also, as noted earlier, the lightning attachment point might not be exactly 15 or 30 m from the antenna; a factor that is more likely to influence the standard deviation than the mean value.

[20] Note that for the current and the magnetic fields and their derivatives, the polarity of the waveforms is ignored and only absolute values are given in the histograms and tables presented here. Note also that the leader contributes to the initial part of the magnetic field and field derivative

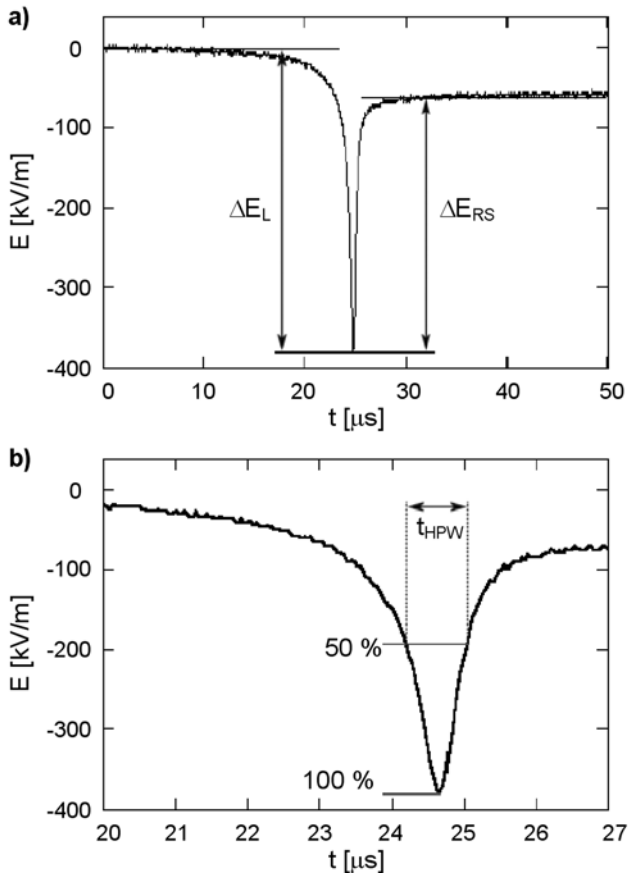

Figure 14. Electric field at 15 m of return stroke 1 of flash S9925 on a) 50 μs and b) 7 μs timescales. The electric field change due to the leader, ΔE_L, and electric field change due to the return stroke, ΔE_{RS}, are illustrated in a). The width of the electric field pulse, t_{HPW}, was measured at $0.5\Delta E_L$, as illustrated in b). Atmospheric electricity sign convention.

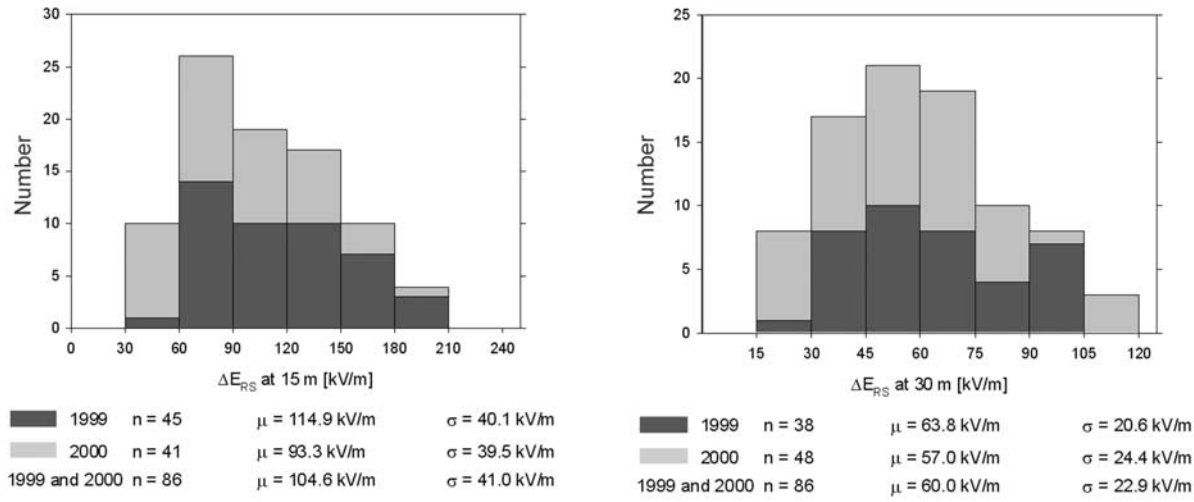

Figure 15. Histograms of return-stroke electric field changes.

waveforms, resulting in a ramp in the beginning of these waveforms (see Figures 21 and 25).

[21] A 30–90% risetime is measured and presented for the magnetic fields and field derivatives of the return stroke since that risetime contains little if any contamination from the leader and is therefore more appropriate than the widely used 10–90%. In addition to giving 30–90% risetime for the return stroke magnetic fields and field derivatives, for consistency and comparison we use this risetime for the other current and electric field and field derivative waveforms.

[22] The histograms presented in this section include the sample size n, the arithmetic mean μ, and the standard deviation σ from the data sets obtained in 1999 and 2000, separately and combined.

3.1. Current and Current Derivative

[23] An example of a measured current waveform is shown in Figure 6 and an example of a measured current derivative waveform in Figure 7. The peak immediately following the sharp rise was chosen to determine $t_{30-90\%}$ if the waveform after this peak was more or less flat, as shown in Figures 6 and 7, even if the actual peak value occurred later. In our view, this approach (also used for the electric field derivative dE/dt and the magnetic flux density B and its derivative dB/dt) provides the most meaningful information about the risetime. Histograms of current peak, current 30–90% risetime, and current half-peak width are found in Figures 8, 9, and 10, respectively. Histograms of current derivative peak, 30–90% risetime, and half-peak width are found in Figures 11, 12, and 13, respectively. Thirteen current derivative peaks in the 1999 data were obtained by differentiating the measured current waveform; all others were directly measured.

3.2. Electric Field

[24] An example of the electric field from a triggered lightning stroke (dart leader/return stroke sequence) is shown in Figure 14. The zero field in Figure 14 is arbitrarily set at the beginning of the 50 μs measurement window. We compared long duration E-field records with

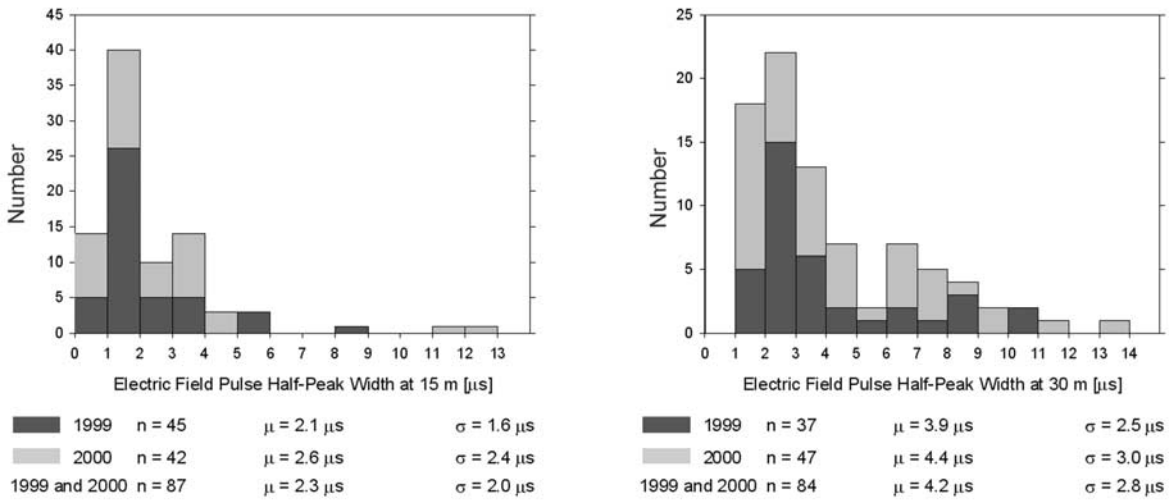

Figure 16. Histograms of leader/return stroke electric field pulse widths.

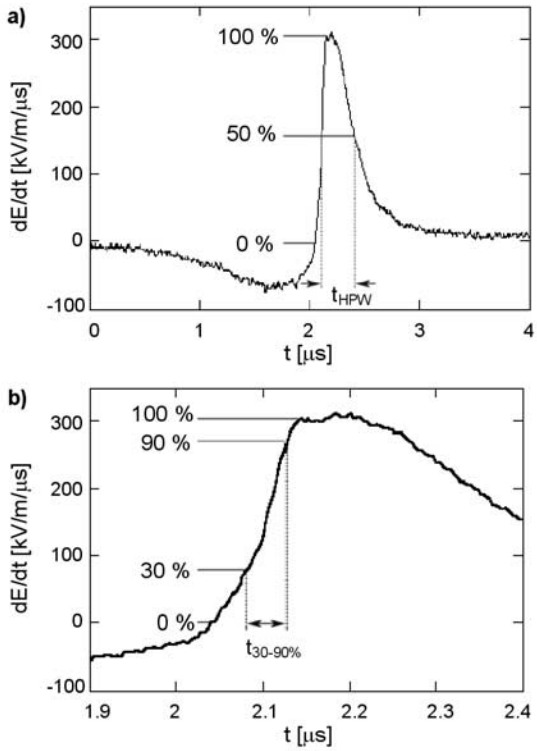

Figure 17. Electric field derivative of event S9932, return stroke 1 on a) 4 μs and b) 0.5 μs timescales. Half-peak width and 30–90% risetime measurements are illustrated in a) and b), respectively. Atmospheric electricity sign convention.

our 50 μs E-field record and found that there is typically little E-field change prior to the 50 μs time window. The negative (atmospheric electricity sign convention) excursion of the waveform ΔE_L due to the descending dart leader is followed by the positive field change ΔE_{RS} due to the ascending return stroke [e.g., *Rubinstein et al.*, 1995]. Histograms of the return stroke field change at 15 m and at 30 m are found in Figure 15 and histograms of the width of the leader/return stroke electric field pulse (Figure 14) at half of leader field change in Figure 16. For pairs of return stroke field changes measured simultaneously at 15 m and 30 m, the mean ratio for 78 events was 1.75 with a standard deviation of 0.13.

3.3. Electric Field Derivative

[25] The electric field derivative measured at close range typically exhibits a bipolar waveform with the initial negative (atmospheric electricity sign convention) part being due to the descending leader and the following positive part due to the ascending return stroke [e.g., *Uman et al.*, 2000]. Figure 17 shows an example of a dE/dt waveform and illustrates the measurements of the 30–90% risetime, $t_{30-90\%}$, and the half-peak width, t_{HPW}. Note that the peak value used to determine the 30–90% risetime was chosen at the end of the sharp rising edge of the dE/dt waveform (see section 3.1). The zero field is set at the beginning of the 10 μs measurement window, which has 5 μs of pretrigger. At this time the waveform is essentially flat. Histograms of the dE/dt peak values are presented in Figure 18. Histograms of the electric field derivative 30–90% risetime and half-peak width are presented in Figures 19 and 20, respectively.

3.4. Magnetic Field

[26] Figure 21 shows an example of a magnetic field waveform measured at 15 m. Histograms of the peak magnetic flux density are given in Figure 22. The peak value used to determine the 30–90% risetime was chosen at the end of the sharp rising edge of the magnetic field waveform (see section 3.1). Note that the magnetic field peak, which is attributed to the return stroke, may include a small contribution from the leader [*Schnetzer et al.*, 1998]. Histograms of the 30–90% risetime of the magnetic field waveform and of the half-peak width are found in Figures 23 and 24, respectively.

3.5. Magnetic Field Derivative

[27] An example of a magnetic field derivative waveform at 15 m is shown in Figure 25. Histograms are presented for the following parameters defined in Figure 25: peak value

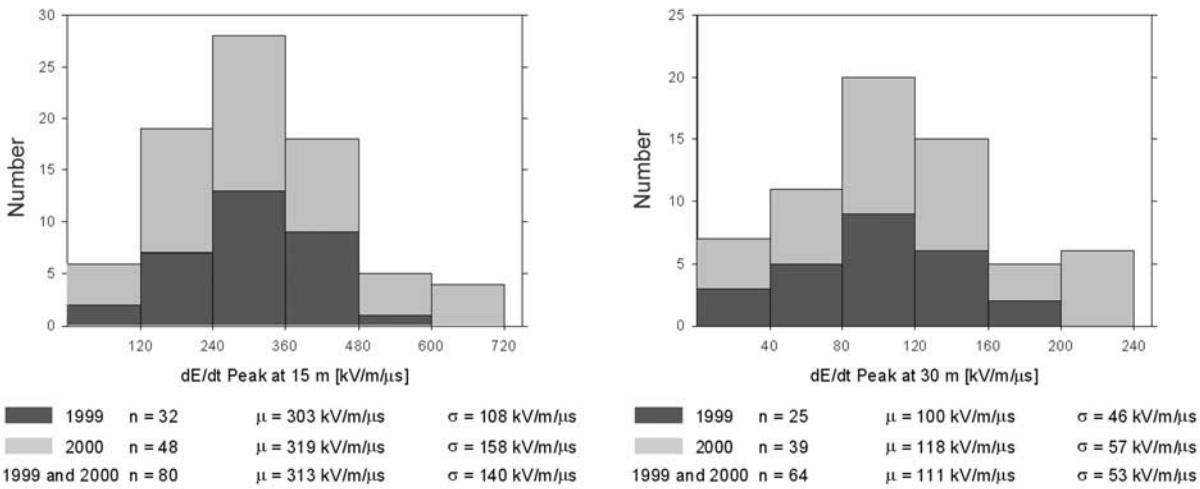

Figure 18. Histograms of return-stroke electric field derivative peaks.

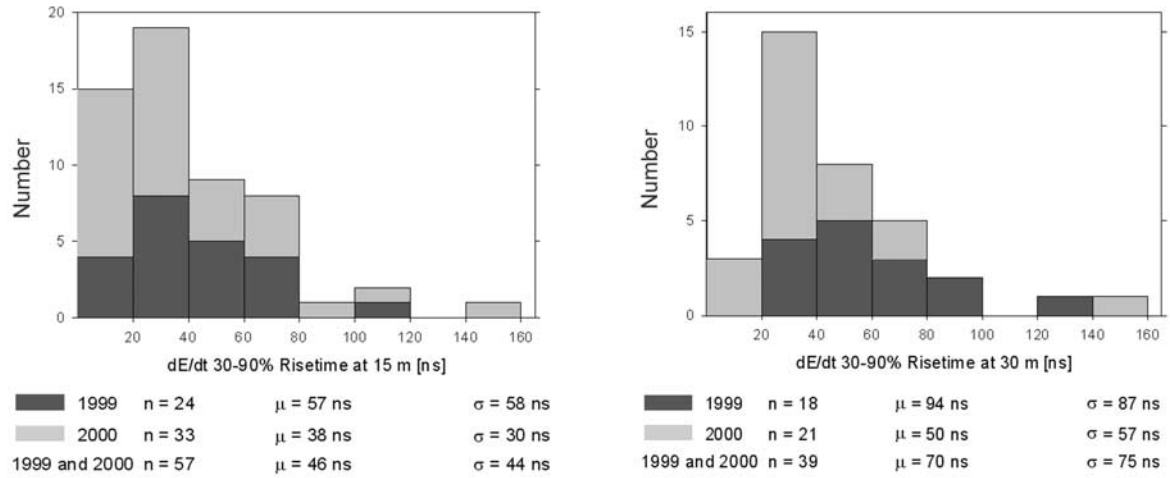

Figure 19. Histograms of dE/dt risetimes. The 15 m data contain 2 values at 210 ns and 250 ns not shown in the histograms but included in the statistics for 1999. The 30 m data contain 4 values, 240 ns, 250 ns and 330 ns (1999), and 270 ns (2000), not shown in the histograms but included in the statistics.

(Figure 26), 30–90% risetime (Figure 27), and width at half of peak value (Figure 28).

4. Discussion

[28] There have been a number of previous measurements of triggered lightning return stroke current characteristics [e.g., *Weidman et al.*, 1986; *Leteinturier et al.*, 1991; *Fisher et al.*, 1993; *Depasse*, 1994; *Crawford*, 1998; *Rakov et al.*, 1998; *Uman et al.*, 2000] with which our data on current can be compared. That comparison is found in Table 1, where n denotes the sample size, min./max. the minimum/maximum values, σ the standard deviation, and σ_{log} the standard deviation of the logarithm (base 10) of the parameter. The same notation is used in Tables 2–6. A relatively low resistance grounding was used in our 1999 and 2000 experiments (6 Ω) and, according to *Rakov et al.* [1998], in the experiments conducted by *Fisher et al.* [1993] in 1990 at the KSC (0.12 Ω) and in 1991 in Alabama. The grounding resistance in the experiments conducted at Saint-Privat d'Allier, France, in 1990 and 1991 was 9 Ω [*Depasse*, 1994], also relatively low, and at Camp Blanding in 1997 was 220 Ω [*Crawford*, 1998] and in 1998 was 58 Ω or 350 Ω [*Uman et al.*, 2000]. The grounding resistance in the 1993 experiment at Camp Blanding was initially very high (tens of kilo-ohms [*Rakov et al.*, 1998]), but was probably lowered considerably once the lightning channel attached to one of the three coaxial cables buried 1 m beneath the ground surface.

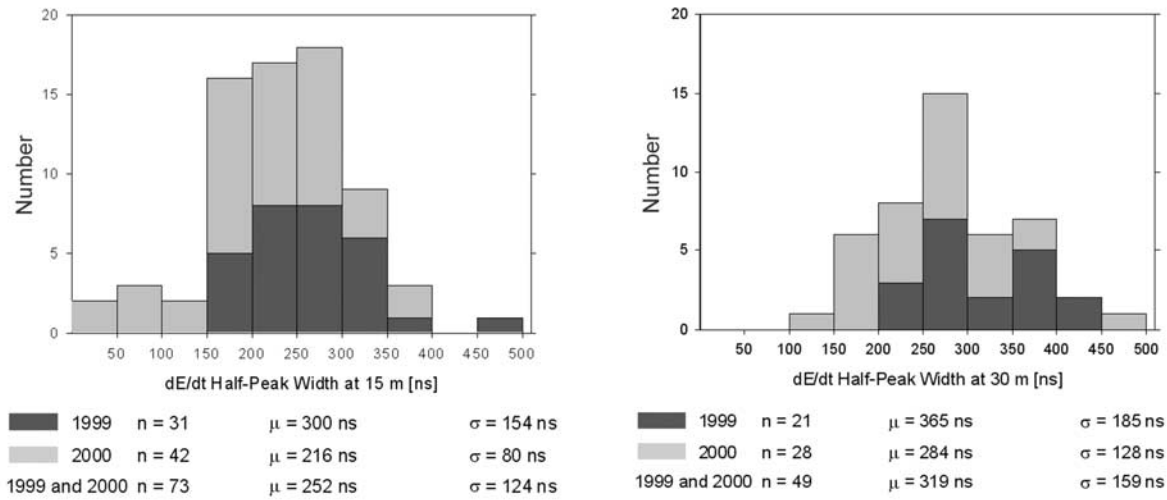

Figure 20. Histograms of dE/dt half-peak widths. The 15 m data contain 2 values at 750 ns and 880 ns (1999) not included in the histograms. The 30 m data contain 2 values at 880 ns and 900 ns (1999) not included in the histograms. These measurements not shown in the histograms are included in the statistics.

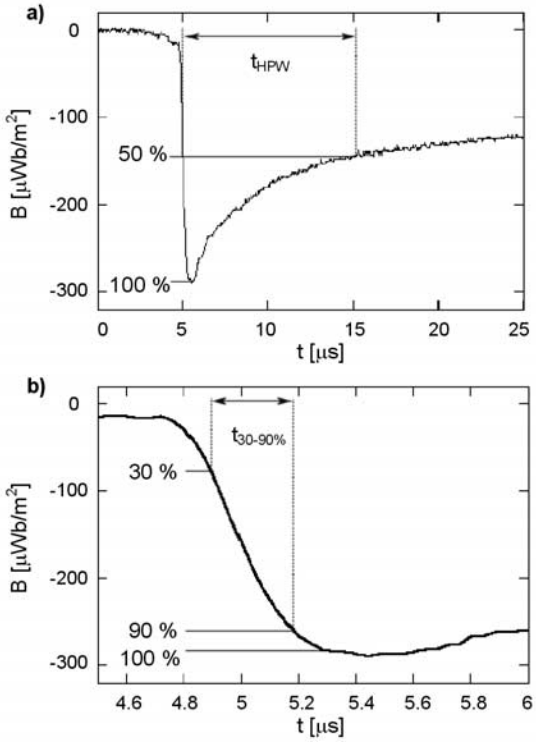

Figure 21. Magnetic field at 15 m of return stroke 3 of flash S9918 on a) 25 μs and b) 1.5 μs timescales. Half-peak width and 30–90% risetime measurements are illustrated in a) and b), respectively.

[29] The arithmetic mean of 64 current peaks measured at Camp Blanding in 1999 and 2000 is 16.2 kA (maximum value 36.8 kA, σ = 7.6 kA). *Depasse* [1994] reports a slightly lower arithmetic mean of 14.3 kA (maximum value 60 kA, σ = 9.0 kA) for 305 values measured at the Kennedy Space Center (KSC), Florida and a lower arithmetic mean of 11.0 kA (maximum value 49.9 kA, σ = 5.6 kA) for 54 values measured at Saint-Privat d'Allier, France. *Fisher et al.* [1993] found a geometric mean of 12 kA (σ_{log} = 0.28), which is somewhat lower than the geometric mean found in our 1999–2000 data (14.2 kA). Note that *Fisher et al.*'s [1993] value of 12 kA is for combined data obtained by them in 1990 at the KSC (8 values) and in 1991 at Fort McClellan, Alabama (37 values), the individual GM values being 15 kA and 11 kA, respectively. *Rakov et al.* [1998], *Crawford* [1998], and *Uman et al.* [2000] report an arithmetic mean of 15.1 kA (n = 37, max. = 44.4 kA, σ = 9.0 kA), 12.8 kA (n = 11, max. = 22.6 kA, σ = 5.6 kA), and 14.8 kA (n = 25, max. = 33.2 kA, σ = 7.0 kA) from measurements at Camp Blanding in 1993, 1997, and 1998, respectively. The generally higher arithmetic mean in our 1999–2000 data might be attributable to the relatively high trigger threshold (5 kA) in our 1999 experiment. *Depasse* [1994] and *Fisher et al.* [1993] report that at least 5% of their currents were below 5 kA. Dependencies of peak current on lower measurement limit were studied by *Rakov* [1985], on grounding conditions by *Depasse* [1994], on trigger threshold level and on grounding conditions by *Rakov et al.* [1998], and on triggering structure height by *Rakov* [2001]. *Depasse* [1994] hypothesized a dependence between peak current and grounding resistance, based on a comparison of the data collected between 1985 and 1991 at the KSC (grounding resistance values 0.1–0.15 Ω) with the data collected between 1986 and 1991 at Saint-Privat d'Allier, France (grounding resistance of 9 Ω). *Rakov et al.* [1998] could not find such a dependence using various data sets obtained at the KSC, Fort McClellan, and Camp Blanding, where the grounding resistance ranged from 0.1 Ω to more than hundreds of ohms.

[30] A comparison of peak current statistics obtained at Camp Blanding in 1993, 1997, 1998, and 1999–2000 shows that the 1999–2000 data are characterized by the highest arithmetic and geometric means. This could be attributable to the lower grounding resistance in our 1999–2000 experiment compared to all earlier Camp Blanding experiments, although some bias towards larger values in our data might be due to the relatively high current threshold in our 1999 experiment, as noted earlier. Note that in the comparison of the several Camp Blanding experiments any variations due to different storm types and local topography are minimized relative to comparisons of results from different geographical locations. Although a tendency

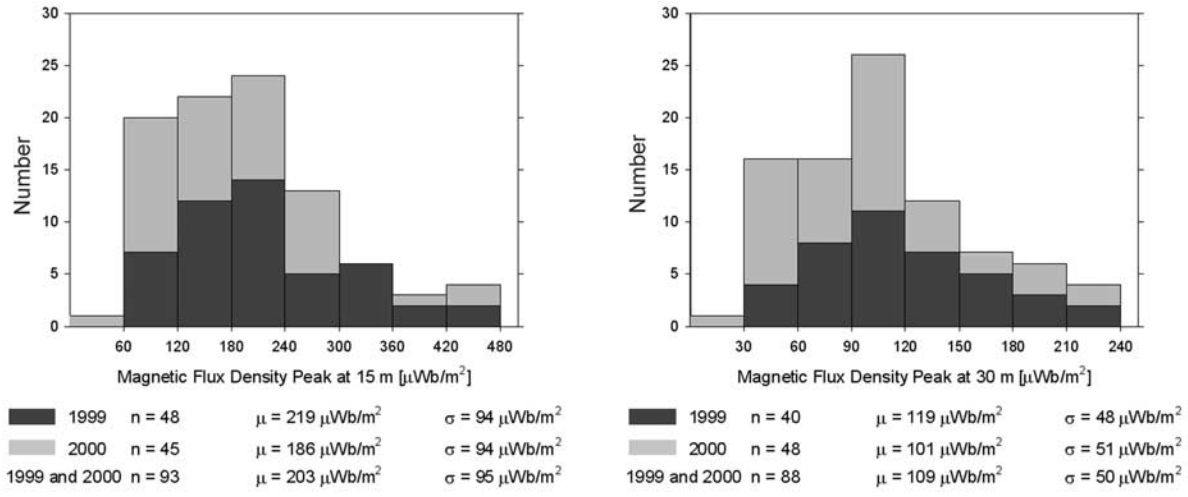

Figure 22. Histograms of magnetic flux density peaks.

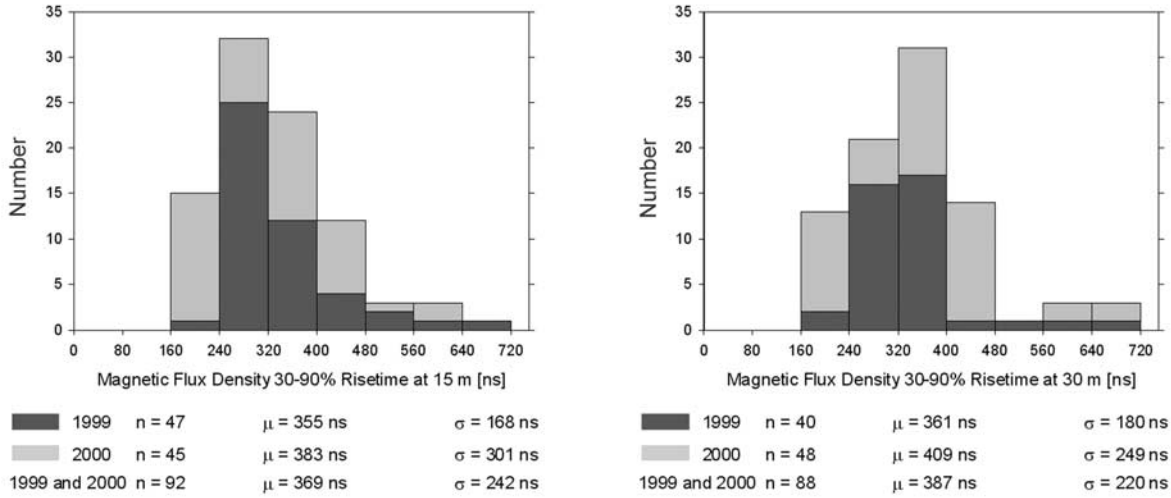

Figure 23. Histograms of magnetic flux density risetimes. The 15 m data contain 2 values, 1280 ns (1999) and 2250 ns (2000), not shown in the histograms. The 30 m data contain 2 values, 1320 ns (1999) and 1890 ns (2000), not shown in the histograms. These measurements not shown in the histograms are included in the statistics.

for larger current peaks to be associated with better grounding might be inferred from the comparison of Camp Blanding measurements in different years, it could actually be due to other factors. For instance, our peak current arithmetic means were 19.5 kA (n = 27) in 1999 and 13.8 kA (n = 37) in 2000 (Figure 8) and the corresponding geometric means were 18.0 kA and 12.4 kA, that is, the year-to-year variation for the same grounding conditions is greater than between the 2000 data set and any other Camp Blanding data set obtained under poorer grounding conditions. The large difference between the peak current means in 1999 and 2000 cannot be attributed to the different triggering threshold (5 kA in 1999 and 3.2 kA in 2000), because none of the current peaks recorded in 2000 were less than 5 kA. It appears that the sample sizes for peak current measurements, n = 27 for the 1999 experiment and n = 37 for the 2000 experiment, are insufficient to obtain statistically reliable mean values that converge towards the population mean, although the natural year-to-year variation might conceivably be more important than the number of measurements in each given year.

[31] The arithmetic mean of the current half-peak width (HPW) of 13.2 μs for 64 current waveforms measured at Camp Blanding in 1999–2000 is significantly lower than that found by *Depasse* [1994] of 49.8 μs for 24 current waveforms at Saint-Privat d'Allier, and by *Crawford* [1998] of 35.7 μs for 11 waveforms measured at Camp Blanding in 1997. Further, our geometric mean HPW is lower than the KSC/Alabama value of *Fisher et al.* [1993]. Also, our current 30–90% risetimes are less than those measured by *Fisher et al.* [1993], as evident in Table 1. It follows from the above that our current wave shapes are apparently

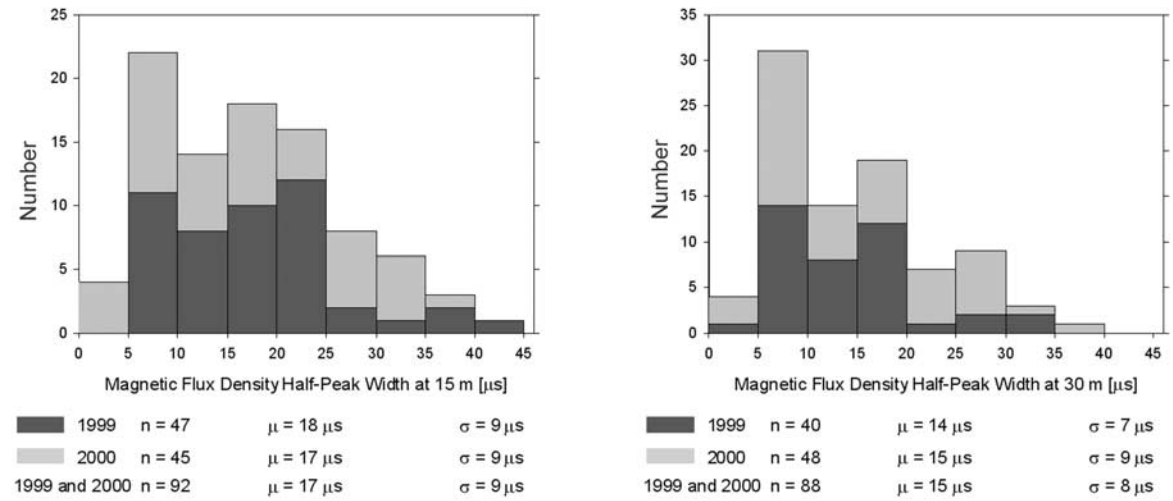

Figure 24. Histograms of magnetic flux density half-peak widths.

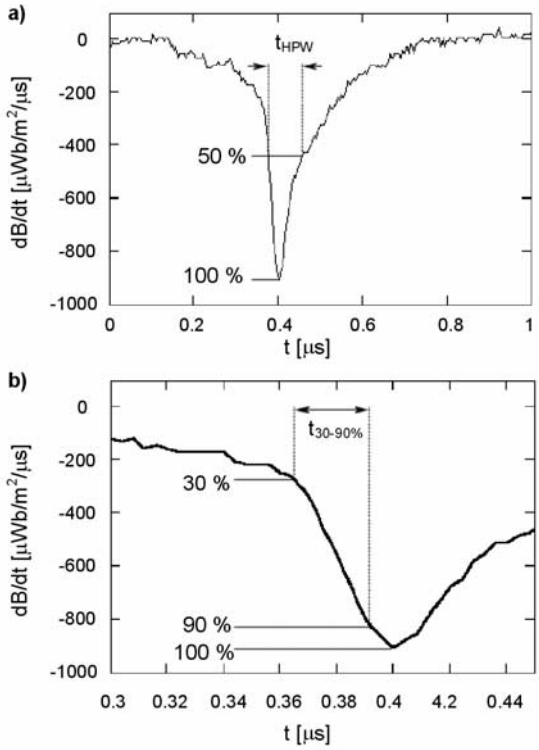

Figure 25. Magnetic field derivative at 15 m of return stroke 6 of flash S9933 on a) 1 μs and b) 0.15 μs timescales. Half-peak width and 30–90% risetime measurements are illustrated in a) and b), respectively.

"sharper" than the current wave shapes observed by others. Perhaps, the relatively low grounding resistance (6 Ω) of our grounding grid resulted in the sharper current peaks, although for an even better grounded (0.12 Ω) but relatively tall (20 m) tower at KSC *Fisher et al.* [1993] reported for 8 events a geometric mean HPW of 23 μs, a factor of two or so larger than the 10.5 μs in our data.

[32] *Leteinturier et al.* [1990, 1991], *Depasse* [1994], and *Uman et al.* [2000] present directly measured triggered lightning return stroke current derivative characteristics. Statistics on dI/dt peaks from all other triggered-lightning studies were obtained from evaluating the slope of the measured current rise toward peak, a technique that usually underestimates the current derivative peak due to bandwidth limitations of the current sensor and the recording device [*Leteinturier et al.*, 1991]. Table 2 shows a comparison of the current derivative data from *Depasse* [1994], *Uman et al.* [2000], and our 1999–2000 current derivative data. We found an arithmetic mean of 117 kA/μs (maximum value 292 kA/μs, σ = 65 kA/μs). Comparing the 12 current derivative peaks directly measured in 1999 (dI/dt_{direct}) with the peak values obtained from differentiating the measured currents of the same stroke ($dI/dt_{indirect}$) we found that 5 $dI/dt_{indirect}$ peaks deviate about ±10% from the corresponding dI/dt_{direct} peaks and 7 $dI/dt_{indirect}$ peaks deviate between −10% and −20% from the corresponding dI/dt_{direct} peaks. This implies that the 13 dI/dt peaks obtained from differentiating measured currents are likely to be underestimated. Note that the largest dI/dt value in our data, 292 kA/μs, was obtained by differentiating a measured current waveform and, in view of the discussion above, that value is possibly underestimated. *Depasse* [1994] found an arithmetic mean of 118 kA/μs (maximum value 411 kA/μs, σ = 97 kA/μs), similar to ours, for 134 values measured at the Kennedy Space Center, Florida and a considerably lower arithmetic mean of 43 kA/μs (maximum value 139 kA/μs, σ = 25 kA/μs) for 47 values measured at Saint-Privat d'Allier, France. According to *Depasse* [1994], the relatively low arithmetic mean of the current derivative peaks measured at Saint-Privat d'Allier might be attributable to errors in the Saint-Privat d'Allier current derivative measurement. *Uman et al.* [2000] report an arithmetic mean of 80 kA/μs (maximum value 152 kA/μs, σ = 35 kA/μs) for 15 values of dI/dt obtained by differentiating currents measured at Camp Blanding in 1998.

[33] *Depasse* [1994] presents electric fields measured at 50 and 77 m at Saint-Privat d'Allier. Electric fields due to triggered-lightning leader/return stroke sequences measured at distances between 10 and 621 m in 1993 to 1999 at Camp Blanding have been analyzed by *Rakov et al.* [1998],

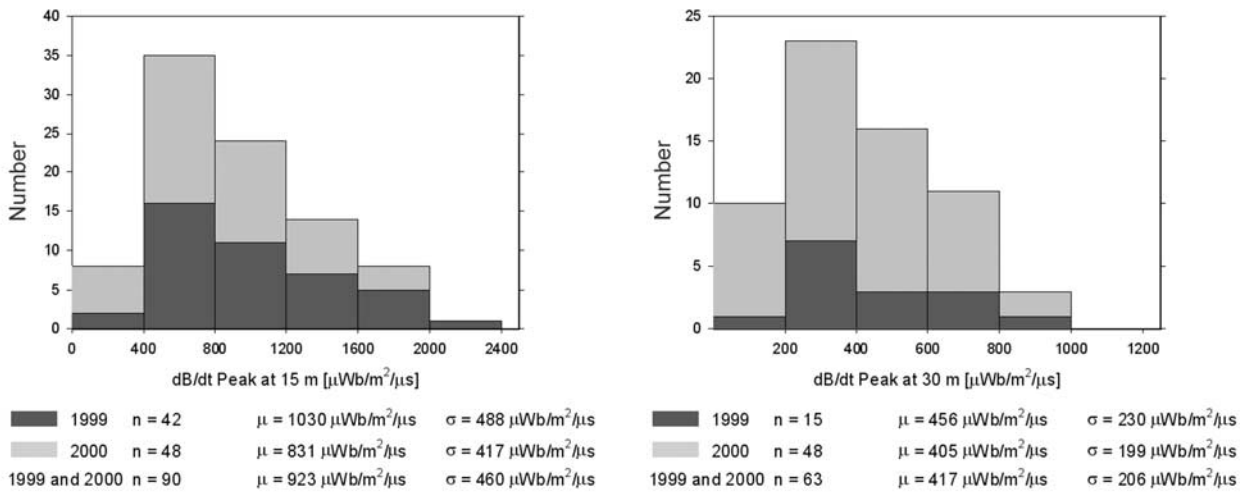

Figure 26. Histograms of dB/dt peaks.

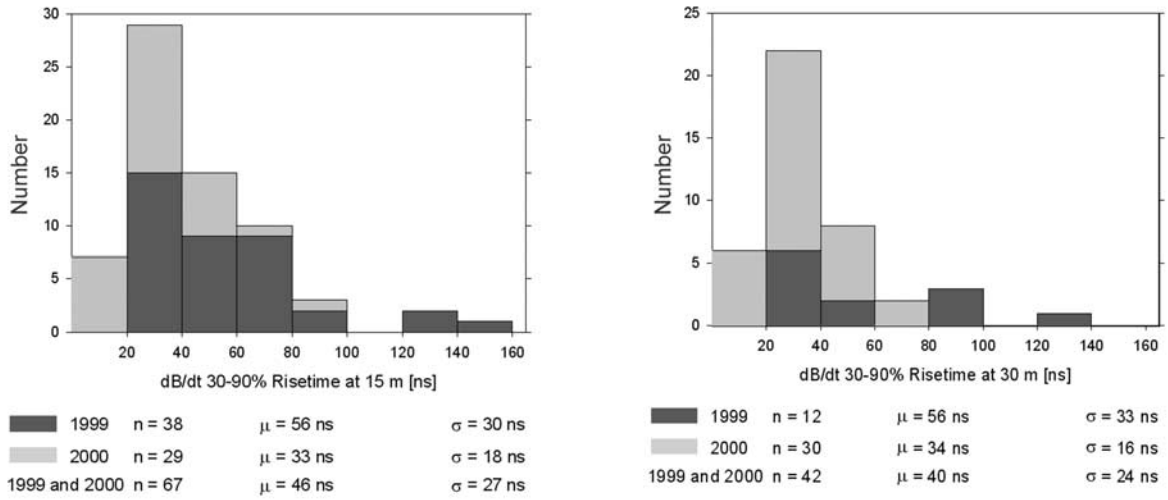

Figure 27. Histograms of dB/dt risetimes.

Crawford [1998], and *Crawford et al.* [2001]. Some of these published electric field statistics for triggered lightning are compared to those of the present study in Table 3. The arithmetic mean of the ratio between 76 leader electric field changes simultaneously measured at 15 m and 30 m at Camp Blanding in 1999 and 2000 is 1.88 (σ = 0.15), suggesting a distance dependence of $r^{-0.9}$, on average. The arithmetic mean of the ratio between 77 return stroke electric field changes simultaneously measured at 15 m and 30 m at Camp Blanding in 1999 and 2000 is 1.76 (σ = 0.18), suggesting a distance dependence of $r^{-0.8}$, on average. *Crawford et al.* [2001] generally observed an r^{-1} distance dependence of the leader electric field changes between 10 and 621 m, with a few exceptions, a result which implies a uniform charge distribution on the lower kilometer or so of the leader channel [*Rubinstein et al.*, 1995]. The apparent discrepancy between Crawford et al.'s distance relationship and ours could be due to the fact that in our experiment at very close distances (15 and 30 m) the lightning channel geometry has a greater effect on the fields than in the 10–621 m distance range, and that lightning sometimes did not attach to the strike rod but to the rocket launcher or pit edge (in 1999), or the metal ring (in 2000), strike points that change the ratio of the distances to the sensors from the ideal value of two. On the other hand, for a subset of 38 events in our 1999 data set, *Crawford et al.* [2001] reported a mean value of the ratio of 2.0 with the range of variation being from 1.5 to 2.4. Also, *Crawford et al.* [2001] noted that the distance dependence was slightly weaker at closer ranges and attributed this to the possible effect of the metallic launcher, lightning channel geometry, variation of charge density with height, or limited sample size. Finally, it is worth noting that *Crawford et al.* [2001] studied the leader field change while we present statistics on the return-stroke field change and that, while the two field changes are usually similar, there is sometimes an appreciable difference between them (see Figure 14).

[34] The arithmetic mean of our electric field pulse half-peak widths measured at 15 and 30 m is 2.3 μs (n = 87) and 4.2 μs (n = 84), respectively. The ratio between 75 half-peak

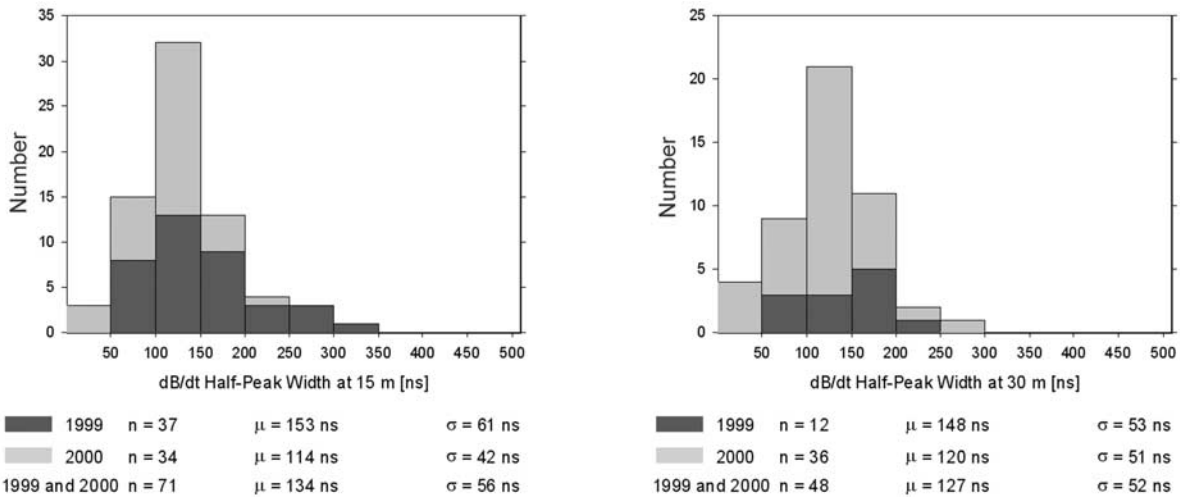

Figure 28. Histograms of dB/dt half-peak widths.

Table 1. Comparison of Current Data for Negative Rocket-Triggered Lightning[a]

Location/Year	n	Min.	Max.	Arithmetic Mean	σ	Geometric Mean	σ_{log}	Reference[b]
Current Peak, kA								
Kennedy Space Center, Florida; 1985–1991	305	2.5	60.0	14.3	9.0	-	-	1
Saint-Privat d'Allier, France; 1986, 1990–1991	54	4.5	49.9	11.0	5.6	-	-	1
Kennedy Space Center, Florida and Fort McClellan, Alabama; 1990, 1991	45	-	-	-	-	12	0.28	2
Camp Blanding, Florida; 1993	37	5.3	44.4	15.1	-	13.3	0.23	3
Camp Blanding, Florida; 1997	11	5.3	22.6	12.8	5.6	11.7	0.20	4
Camp Blanding, Florida; 1998	25	5.9	33.2	14.8	7.0	13.5	0.19	5
present study	64	5	36.8	16.2	7.6	14.5	0.21	
Current 10–90% Risetime, ns								
Kennedy Space Center, Florida and Fort McClellan, Alabama; 1990, 1991	43	-	-	-	-	370	0.29	2
Saint-Privat d'Allier, France; 1990–1991	37	250	4900	1140	1100	-	-	1
Camp Blanding, Florida; 1997	11	300	4000	900	1200	600	0.39	4
Current 30–90% Risetime, ns								
Kennedy Space Center, Florida and Fort McClellan, Alabama; 1990, 1991	43	-	-	-	190	280	0.28	2
present study	65	54	1751	260	316	191	0.29	
Current Half-Peak Width, μs								
Saint-Privat d'Allier, France; 1990–1991	24	14.7	103.2	49.8	22.4	-	-	1
Kennedy Space Center, Florida and Fort McClellan, Alabama; 1990, 1991	41	-	-	-	-	18	0.30	2
Camp Blanding, Florida; 1997	11	6.5	100	35.7	24.6	29.4	0.29	4
present study	64	2.4	37.2	13.2	8.5	10.5	0.32	

[a]The polarity of the peak values is ignored.
[b]References: 1, *Depasse* [1994]; 2, *Fisher et al.* [1993]; 3, *Rakov et al.* [1998]; 4, *Crawford* [1998]; 5, *Uman et al.* [2000].

widths measured simultaneously at 30 and 15 m is 1.93, which corresponds to a distance dependence close to linear ($r^{0.95}$). *Rakov et al.* [1998] previously found a distance dependence close to linear for the electric field half-peak widths of 9 strokes simultaneously measured at 30, 50, and 110 m.

[35] *Depasse* [1994] presents statistics on electric field derivatives measured at 50 m at Saint-Privat d'Allier.

Table 2. Comparison of Current Derivative Data for Negative Rocket-Triggered Lightning[a]

Location/Year	n	Min.	Max.	Arithmetic Mean	σ	Geometric Mean	σ_{log}
dI/dt Peak, kA/μs							
Kennedy Space Center, Florida; 1985–1991[b]	134	5	411	118	97	-	-
Saint-Privat d'Allier, France; 1986, 1990–1991[b]	47	13	139	43	25	-	-
Camp Blanding, Florida; 1998[c]	15	45	152	80	35	73	0.17
present study[d]	64	8	292	117	65	97	0.31
dI/dt 30–90% Risetime, ns							
present study	29	17	69	32	13	30	0.16
dI/dt 10–10% Width, ns							
Saint-Privat d'Allier, France; 1990–1991[b]	17	70	2010	400	210	-	-
dI/dt Half-Peak Width, ns							
present study	29	49	149	92	25	89	0.12

[a]The polarity of the peak values is ignored.
[b]*Depasse* [1994].
[c]*Uman et al.* [2000].
[d]Fifteen dI/dt peaks obtained from differentiating I.

Table 3. Comparison of Electric Field Data for Negative Rocket-Triggered Lightning

Location/Year	Distance	n	Min.	Max.	Arithmetic Mean	σ	Geometric Mean	σ_{log}
Return Stroke Electric Field Change, kV/m								
Saint-Privat d'Allier, France; 1990–1991[a]	50 m	14	14.5	41.9	26.0	9.0	-	-
Saint-Privat d'Allier, France; 1990–1991[a]	77 m	13	11.4	25.2	17.5	5.5	-	-
Camp Blanding, Florida; 1997[b]	10 m	10	28.1	294.7	109.5	73.4	91.6	0.28
Camp Blanding, Florida; 1997[b]	30 m	10	11.4	50.2	31.1	13.0	28.3	0.21
present study	15 m	86	30.2	197.2	104.6	41.0	96	0.19
present study	30 m	86	16.3	116.2	60.0	22.9	55.3	0.19
Electric Field Half-Peak Width, μs								
Camp Blanding, Florida; 1993[b]	30 m	6	2.2	8.5	4.6	3.0	3.8	0.28
Camp Blanding, Florida; 1993[b]	50 m	6	3.5	15	7.7	5.3	6.3	0.28
Camp Blanding, Florida; 1993[b]	110 m	6	7.3	30	15.3	10.9	12.5	0.29
Camp Blanding, Florida; 1997[b]	10 m	9	1	34.2	7.2	10.9	3.2	0.54
Camp Blanding, Florida; 1997[b]	30 m	9	1.4	11.2	4.0	3.2	3.2	0.30
present study	15 m	87	0.8	12.2	2.3	2.0	1.9	0.28
present study	30 m	84	1.4	13.9	4.2	2.8	3.5	0.26

[a]*Depasse* [1994].
[b]*Crawford* [1998].

Electric field derivatives due to triggered-lightning leader/return stroke sequences have been studied for distances of 10, 14, and 30 m by *Uman et al.* [2000], as noted in section 1. A comparison of these data sets with our 1999–2000 data is found in Table 4. Note that the means of the dE/dt peaks in the data of *Uman et al.* [2000] are biased towards lower values, since four dE/dt measurements at 10 m were saturated at 270 kV/m and three dE/dt measurements at 30 m were saturated at 170 kV/m. The saturated data are not included in the statistics of *Uman et al.* [2000]. For our 1999 and 2000 data the arithmetic mean of the ratio between 60 return stroke dE/dt peaks simultaneously measured at 15 and 30 m is 2.89 (σ = 0.37). It can be inferred that the distance variation of the dE/dt peaks between 15 and 30 m is $r^{-1.5}$, on average. This observation is in contrast to the results of a similar analysis given by *Uman et al.* [2000] for distances of 10 and 30 m. In their data, the arithmetic mean of the ratio between 5 return stroke dE/dt peaks simultaneously measured at 10 and 30 m was 1.77, resulting in a distance dependence of $r^{-0.5}$, on average. The reason for the difference between the distance dependence inferred from the 1999 and 2000 data and the distance dependence

Table 4. Comparison of Electric Field Derivative Data for Negative Rocket-Triggered Lightning

Location/Year	Distance	n	Min.	Max.	Arithmetic Mean	σ	Geometric Mean	σ_{log}
dE/dt Peak, kV/m/μs								
Saint-Privat d'Allier, France; 1990–1991[a]	50 m	14	5	144	82	18	-	-
Camp Blanding, Florida; 1998	10 m	7	142	260	209	40	205	0.09
Camp Blanding, Florida; 1998	14 m	4	84	299	191	89	173	0.23
Camp Blanding, Florida; 1998[b]	30 m	7	107	226	144	44	139	0.12
present study	15 m	80	37	657	313	140	273	0.26
present study	30 m	64	19	234	114	53	95	0.27
dE/dt 30–90% Risetime, ns								
present study	15 m	57	12	250	46	44	35	0.30
present study	30 m	39	18	330	70	75	49	0.34
dE/dt 0–100% Risetime, ns								
Camp Blanding, Florida; 1998[b]	10 m	7	30	80	59	20	55	0.18
Camp Blanding, Florida; 1998[b]	14 m	4	40	180	100	63	85	0.29
Camp Blanding, Florida; 1998[b]	30 m	7	50	170	86	44	78	0.19
dE/dt 10–10% Width, ns								
Saint-Privat d'Allier, France; 1990–1991[a]	50 m	12	140	2310	870	860	-	-
dE/dt Half-Peak Width, ns								
Camp Blanding, Florida; 1998[b]	10 m	7	30	490	159	150	118	0.35
Camp Blanding, Florida; 1998[b]	14 m	4	60	510	235	200	174	0.40
Camp Blanding, Florida; 1998[b]	30 m	7	60	180	106	40	101	0.16
present study	15 m	73	41	876	252	124	227	0.21
present study	30 m	49	138	899	319	159	294	0.16

[a]*Depasse* [1994].
[b]*Uman et al.* [2000].

Table 5. Comparison of Magnetic Field Data for Negative Rocket-Triggered Lightning[a]

Location/Year	Distance	n	Min.	Max.	Arithmetic Mean	σ	Geometric Mean	σ_{log}
Magnetic Field Peak, μWb/m²								
Camp Blanding, Florida; 1997[b]	5.5 m	11	150	874	470	223	418	0.23
Camp Blanding, Florida; 1997[b]	10.3 m	10	91	377	230	93	212	0.19
present study	15 m	93	53	466	203	95	182	0.21
present study	30 m	88	27	239	109	50	98	0.21
Magnetic Field 10–90% Risetime, ns								
Camp Blanding, Florida; 1997[b]	5.5 m	11	300	2700	780	770	580	0.31
Camp Blanding, Florida; 1997[b]	10.3 m	10	300	3200	820	910	580	0.34
Magnetic Field 30–90% Risetime, ns								
present study	15 m	92	212	2250	369	242	337	0.16
present study	30 m	88	209	1890	387	220	357	0.16
Magnetic Field Half-Peak Width, μs								
Camp Blanding, Florida; 1997[b]	5.5 m	11	7.7	65.8	25.8	15.2	22.5	0.24
Camp Blanding, Florida; 1997[b]	10.3 m	10	5.1	78.3	26.2	20.4	20.9	0.31
present study	15 m	92	4.1	43.4	17.4	9.1	14.9	0.25
present study	30 m	88	3.4	37.1	14.6	7.9	12.5	0.25

[a]The polarity of the peak values is ignored.
[b]*Crawford* [1998].

inferred from 1998 data is unknown, but is likely due to irregularities in *Uman et al.*'s [2000] 10 m dE/dt measurements, perhaps due to local ground surface arcing, the narrower system frequency bandwidth (10–20 MHz) used at that distance, an undetected system calibration error, or the effects of the relatively high strike object (see section 1). The 30 m field derivative half-peak widths of *Uman et al.* [2000] (μ = 106 μs, n = 7), obtained in 1998 with a frequency bandwidth of 20 MHz, are considerably smaller than the half peak widths we found in our 1999–2000 data (μ = 319 μs, n = 49). This difference might be due to the relatively small sample size of *Uman et al.*'s [2000] data.

[36] *Crawford* [1998] measured magnetic fields at distances between 5.5 m and 500 m. The statistical parameters for magnetic fields measured at 5.5 m (11 values) and 10.3 m (10 values), the two largest data sets from *Crawford* [1998], are listed in Table 5 and compared with our magnetic field data at 15 and 30 m. The arithmetic mean of the ratio between 85 magnetic field peaks simultaneously measured at 15 and 30 m in 1999 and 2000 at Camp Blanding is 1.90 (σ = 0.14), suggesting a distance dependence of $r^{-0.93}$, on average. The ratio between 10 magnetic field peaks simultaneously measured at 5.5 and 10.3 m by *Crawford* [1998] is 1.84, suggesting a distance dependence of $r^{-0.97}$. Ampere's law of magnetostatics, $B = \mu_0 I/2\pi r$, can be used to obtain a reasonable estimate of the peak current from the measured peak magnetic flux density. For example, for the 1999 data, the directly measured current peaks had an arithmetic mean of 19 kA, a geometric mean of 18 kA, and a standard deviation of 8 kA (n = 27). Using Ampere's law and the magnetic field peaks at 15 m, we find 16 kA, 15 kA, and 7 kA (n = 48), and at 30 m, 18 kA, 16 kA, and 7 kA (n = 40). For individual cases, the current peaks determined from Ampere's law differed from the measured current peaks generally between a few percent and about 20%. Contributing to these differences is the fact that the channels may not be at exactly 15 and 30 m, as previously noted, and are not straight and vertical, as well as a possible contribution from the downward propagating leader to the overall magnetic field peak, but not to the current measured at ground level [*Crawford*, 1998; *Schnetzer et al.*, 1998].

[37] The arithmetic mean of our magnetic field half-peak widths measured at 15 and 30 m is 17.4 μs (n = 92) and 14.6 μs (n = 84), respectively. *Crawford* [1998] found HPW means of 25.8 and 26.2 μs for his magnetic fields measured at 5.5 and 10.3 m, respectively, in 1997 at Camp Blanding. The narrower magnetic field HPW in our 1999–2000

Table 6. Magnetic Field Derivative Data for Negative Rocket-Triggered Lightning[a]

Location/Year	Distance	Sample Size	Min.	Max.	Arithmetic Mean	σ	Geometric Mean	σ_{log}
dB/dt Peak, μWb/m²/μs								
present study	15 m	90	108	2190	923	460	804	0.25
present study	30 m	63	53	921	417	206	361	0.26
dB/dt 30–90% Risetime, ns								
present study	15 m	67	13	151	46	27	39	0.24
present study	30 m	42	15	126	40	24	35	0.23
dB/dt Half-Peak Width, ns								
present study	15 m	71	44	317	134	56	124	0.18
present study	30 m	48	33	259	127	52	116	0.20

[a]The polarity of the peak values is ignored.

experiments might be associated with our lower grounding resistance (resulting in sharper current waveforms), as previously discussed, although the magnetic fields in the two experiments were measured at different distances and could be inherently different.

[38] *Baker et al.* [1987] measured one magnetic field derivative at 60 m in 1986 in New Mexico. The peak value and half-peak width of this measurement were approximately 350 $\mu Wb/m^2/\mu s$ and 125 ns. Our magnetic field derivative data are summarized in Table 6. The arithmetic mean of the ratio between 62 return stroke magnetic field derivative peaks simultaneously measured at 15 and 30 m at Camp Blanding is 2.10 ($\sigma = 0.18$), resulting in a distance dependence of $r^{-1.1}$, on average.

[39] In the present paper we have compared our waveform characteristics with those of all other close triggered lightning experiments. Information on similar measurements of dE/dt from distant natural and distant triggered lightning is reviewed by *Uman et al.* [2000], from which additional comparisons can be made to the present data.

5. Summary

[40] Statistical characteristics of the electric and magnetic fields and their time derivatives 15 and 30 m from rocket-triggered lightning, as well as statistical characteristics of their causative currents and current derivatives, based on measurements in 1999 and 2000 at Camp Blanding, Florida, are presented and compared with those from previous triggered-lightning studies. The results are summarized in the form of histograms in Figures 8–10 (current), 11–13 (dI/dt), 15–16 (E-field), 18–20 (dE/dt), 22–24 (B-field), and 26–28 (dB/dt) and in Tables 1–6.

[41] **Acknowledgments.** This research was supported in part by DOT (FAA) grant 99-G-043 and NSF grants ATM-9726100 and ATM-0003994.

References

Baker, L., R. L. Gardner, A. H. Paxton, C. E. Baum, and W. Rison, Simultaneous measurement of current, electromagnetic fields, and optical emission from a lightning stroke, *Electromagnetics*, *7*, 441–450, 1987.

Baum, C. E., Electromagnetic sensors and measurement techniques, in *Fast Electrical and Optical Measurements*, pp. 73–144, Martinus Nijhoff, Zoetermeer, Netherlands, 1986.

Cooray, V., Effects of propagation on the return stroke radiation fields, *Radio Sci.*, *22*, 757–768, 1987.

Cooray, V., and S. Lundquist, Effects of propagation on the risetimes and the initial peaks of radiation peaks from return strokes, *Radio Sci.*, *18*, 409–415, 1983.

Crawford, D. E., Multiple-station measurements of triggered lightning electric and magnetic fields, Masters thesis, Univ. of Fla., Gainesville, 1998.

Crawford, D. E., V. A. Rakov, M. A. Uman, G. H. Schnetzer, K. J. Rambo, M. V. Stapleton, and R. J. Fisher, The close lightning electromagnetic environment: Dart-leader electric field change versus distance, *J. Geophys. Res.*, *106*, 14,909–14,917, 2001.

Depasse, P., Statistics on artificially triggered lightning, *J. Geophys. Res.*, *99*, 18,515–18,522, 1994.

Fisher, R. J., G. H. Schnetzer, R. Thottappillil, V. A. Rakov, M. A. Uman, and J. D. Goldberg, Parameters of triggered-lightning flashes in Florida and Alabama, *J. Geophys. Res.*, *98*, 22,887–22,902, 1993.

Leteinturier, C., C. Weidman, and J. Hamelin, Current and electric field derivatives in triggered lightning return strokes, *J. Geophys. Res.*, *95*, 811–828, 1990.

Leteinturier, C., J. Hamelin, and A. Eybert-Berard, Submicrosecond characteristics of leader-return-stroke currents, *IEEE Trans. Electromagn. Compat.*, *33*(4), 351–357, 1991.

Miki, M., V. A. Rakov, K. J. Rambo, G. H. Schnetzer, and M. A. Uman, Electric fields near triggered lightning channels measured with Pockels sensors, *J. Geophys. Res.*, *107*(D16), 4277, doi:10.1029/2001JD001087, 2002.

Rakov, V. A., On estimating the lightning peak current distribution parameters taking into account the lower measurement limit, *Elektrichestvo*, *no. 2*, 57–59, 1985.

Rakov, V. A., Transient response of a tall object to lightning, *IEEE Trans. Electromagn. Compat.*, *43*(4), 654–661, 2001.

Rakov, V. A., et al., New insights into lightning processes gained from triggered-lightning experiments in Florida and Alabama, *J. Geophys. Res.*, *103*, 14,117–14,130, 1998.

Rakov, V. A., D. E. Crawford, K. J. Rambo, G. H. Schnetzer, M. A. Uman, and R. Thottappillil, M-component mode of charge transfer to ground in lightning discharges, *J. Geophys. Res.*, *106*, 22,817–22,831, 2001.

Rubinstein, M., F. Rachidi, M. A. Uman, R. Thottappillil, V. A. Rakov, and C. A. Nucci, Characterization of vertical electric fields 500 m and 30 m from triggered lightning, *J. Geophys. Res.*, *100*, 8863–8872, 1995.

Schnetzer, G. H., R. J. Fisher, V. A. Rakov, and M. A. Uman, The magnetic field environment of nearby lightning, paper presented at 24th International Conference on Lightning Protection (ICLP), Staffordshire Univ., Birmingham, England, 14–18 Sept. 1998.

Uman, M. A., and D. K. McLain, Magnetic field of lightning return stroke, *J. Geophys. Res.*, *74*, 6899–6910, 1969.

Uman, M. A., V. A. Rakov, G. H. Schnetzer, K. J. Rambo, D. E. Crawford, and R. J. Fisher, Time derivative of the electric field 10, 14, and 30 m from triggered lightning strokes, *J. Geophys. Res.*, *105*(D12), 15,577–15,595, 2000.

Uman, M. A., J. Schoene, V. A. Rakov, K. J. Rambo, and G. H. Schnetzer, Correlated time derivatives of current, electric field intensity, and magnetic flux density for triggered lightning at 15 m, *J. Geophys. Res.*, *107*(D13), 4160, doi:10.1029/2000JD000249, 2002.

Weidman, C., J. Hamelin, C. Leteinturier, and L. Nicot, Correlated current-derivative (dI/dt) and electric field-derivative emitted by triggered lightning, paper presented at International Conference on Lightning and Static Electricity, Air Force Wright Aeronaut. Lab., Dayton, Ohio, 24–26 June 1986.

V. Kodali, V. A. Rakov, K. J. Rambo, G. H. Schnetzer, J. Schoene, and M. A. Uman, Department of Electrical and Computer Engineering, University of Florida, Gainesville, FL 32611, USA. (jenss@ufl.edu)